Cell Death & Differentiation (2021) 28:1627–1643
https://doi.org/10.1038/s41418-020-00688-6

Cell Death & Differentiation

ARTICLE

Activating transcription factor-4 promotes neuronal death induced by Parkinson's disease neurotoxins and α-synuclein aggregates

Matthew D. Demmings[1,2,3] · Elizabeth C. Tennyson[1,2,3] · Gillian N. Petroff[2,3,4] · Heather E. Tarnowski-Garner[2,3] · Sean P. Cregan[1,2,3,4]

Received: 25 November 2019 / Revised: 13 November 2020 / Accepted: 17 November 2020 / Published online: 4 December 2020

Abstract

Parkinson's disease (PD) is a neurodegenerative disease characterized by the loss of dopaminergic neurons in the substantia nigra resulting in severe and progressive motor impairments. However, the mechanisms underlying this neuronal loss remain largely unknown. Oxidative stress and ER stress have been implicated in PD and these factors are known to activate the integrated stress response (ISR). Activating transcription factor 4 (ATF4), a key mediator of the ISR, and has been reported to induce the expression of genes involved in cellular homeostasis. However, during prolonged activation ATF4 can also induce the expression of pro-death target genes. Therefore, in the present study, we investigated the role of ATF4 in neuronal cell death in models of PD. We demonstrate that PD neurotoxins (MPP+ and 6-OHDA) and α-synuclein aggregation induced by pre-formed human alpha-synuclein fibrils (PFFs) cause sustained upregulation of ATF4 expression in mouse cortical and mesencephalic dopaminergic neurons. Furthermore, we demonstrate that PD neurotoxins induce the expression of the pro-apoptotic factors Chop, Trb3, and Puma in dopaminergic neurons in an ATF4-dependent manner. Importantly, we have determined that PD neurotoxin and α-synuclein PFF induced neuronal death is attenuated in ATF4-deficient dopaminergic neurons. Furthermore, ectopic expression of ATF4 but not transcriptionally defective ATF4ΔRK restores sensitivity of ATF4-deficient neurons to PD neurotoxins. Finally, we demonstrate that the eIF2α kinase inhibitor C16 suppresses MPP+ and 6-OHDA induced ATF4 activation and protects against PD neurotoxin induced dopaminergic neuronal death. Taken together these results indicate that ATF4 promotes dopaminergic cell death induced by PD neurotoxins and pathogenic α-synuclein aggregates and highlight the ISR factor ATF4 as a potential therapeutic target in PD.

Introduction

Parkinson's disease (PD) is the second most common neurodegenerative disorder and is characterized by distinct motor symptoms including bradykinesia, postural rigidity, and resting tremor [1]. The motor impairments in PD result from the progressive loss of dopaminergic neurons in the substantia nigra pars compacta and the associated depletion of striatal dopamine [2]. Unfortunately, there is no cure for PD and while current treatments temporarily ameliorate some of the clinical symptoms, they do not mitigate the underlying degenerative processes.

Numerous studies implicate oxidative stress and endoplasmic reticulum (ER) stress as major factors contributing to dopaminergic neuronal cell death in PD. Indeed, markers of oxidative damage, including DNA damage, lipid peroxidation and aggregates of oxidized proteins have been reported in *post-mortem* brain tissue of PD patients [3, 4].

Edited by J.M. Hardwick

Supplementary information The online version of this article (https://doi.org/10.1038/s41418-020-00688-6) contains supplementary material, which is available to authorized users.

✉ Sean P. Cregan
scregan@robarts.ca

[1] Neuroscience Program, University of Western Ontario, London, ON, Canada

[2] Robarts Research Institute, University of Western Ontario, London, ON, Canada

[3] University of Western Ontario, London, ON, Canada

[4] Department of Physiology and Pharmacology, University of Western Ontario, London, ON, Canada

Furthermore, the neurotoxic agents MPTP and 6-OHDA cause selective loss of dopaminergic neurons in rodents, non-human primates, and humans and are known to act by causing oxidative damage [5]. Interestingly, several familial-linked PD genes, including Parkin, Pink1, and DJ-1 have been implicated in the regulation of mitochondrial function, mitophagy, and ROS production [6–9]. In addition to oxidative stress, deficits in cellular proteostasis pathways associated with the aggregation of misfolded proteins such as α-synuclein are thought to contribute to neurodegeneration in PD [10, 11]. One component of the proteostasis network that is affected in PD is the folding capacity of the endoplasmic reticulum resulting in ER stress and activation of the unfolded protein response (UPR) [12, 13]. Indeed, markers of ER stress are commonly observed in *post-mortem* brain tissue derived from PD patients as well as in a variety of cellular and animal models of PD [14–20].

The integrated stress response (ISR) is a cell signaling pathway that is activated in response to diverse stress stimuli, including oxidative stress and ER stress [21]. The ISR involves the stress specific activation of eIF2α kinases (PERK, PKR, HRI, and GCN2) that phosphorylate the translation initiation factor eIF2α resulting in attenuation of general protein translation and the selective translation of stress responsive mRNAs, including activating transcription factor-4 (ATF4) [22–24]. ATF4 is a member of the ATF/CREB family of basic-region leucine transcription factors and can regulate the expression of genes involved in amino acid metabolism and redox homeostasis that promote cell recovery [25]. However, upon sustained activation ATF4 can also induce the expression of factors that have been implicated in promoting cell death, including CHOP and TRB3 [26–28]. Induction of ATF4 has been reported in cellular and animal models of PD as well as in *post-mortem* brain tissue of PD patients [18, 19, 29]. However, the role of ATF4 in regulating neuronal survival remains controversial. Therefore, in the present study, we investigated the role of ATF4 in primary dopaminergic neurons derived from wildtype and ATF4-deficient mice in neurotoxins (MPP+ and 6-OHDA) and α-synuclein preformed fibrils models of PD.

Materials and methods

Animals

All animal procedures were performed as per guidelines set by the Animal Care Committee at Western University, in accordance with the Canadian Council on Animal Care. Mice carrying an ATF4-null mutation were obtained from Dr. Tim Townes (University of Alabama, Birmingham, AL). ATF4 mice were maintained on a C57BL/6 background and were genotyped as previously described [30]. Mice carrying a targeted null mutation for PUMA were obtained from Dr. Andreas Strasser (WEHI, Melbourne, Australia) and genotyping of these mice was performed as described previously. Wild-type and ATF4 and PUMA knock-out littermates were generated by breeding heterozygous mice.

Primary cortical and mesencephalic neuron culture

Cortical neurons were dissociated from embryonic day 14.5–15.5 male and female embryos and cultured in Neurobasal plus media (ThermoFisher, #A35829-01) supplemented with B27 plus (ThermoFisher, #A35828-01), 0.5× Glutamax (ThermoFisher, #35050-061), and 50 U/mL penicillin: 50 µg/mL streptomycin (PenStrep; ThermoFisher, #15140-122) as previously described [31]. Mesencephalic tissue was obtained using a protocol adapted from Gaven, Marin, and Claeysen [32], neurons were then dissociated and cultured in the same media conditions as cortical neurons.

Drugs treatments

Drug treatments were initiated in cortical and mesencephalic neuronal cultures at 7 DIV unless specified otherwise. Stock solutions of 1-methyl-4-phenylpyridinium iodide (MPP+; Millipore Sigma #D048), 6-hydroxydopamine hydrobromide (6-OHDA; Millipore Sigma #H116), and Sodium Arsenite ($NaAsO_2$; Millipore Sigma #S7400) were prepared in ddH_2O. Stock solutions of Thapsigargin (TG; Millipore Sigma #T9033) and 6,8-dihydro-8-(1H-imidazol-5ylmethylene)-7H-pyrrolo[2,3-g] benzothiazole-7-one [C16] (Tocris #5382) were prepared in DMSO. Drugs were diluted in neuron culture media immediately before administration to cultures at indicated concentrations.

Preparation of human α-synuclein preformed fibrils

Recombinant human α-synuclein monomers (Proteos #RP-003) were used to generate fibrils based on the protocol of Volpicelli-Daley and colleagues [33]. Briefly, monomers were shaken at 1000 rpm (37 °C) for 7 days to produce fibrils and then aliquoted and stored at −80 °C. Aliquots of preformed fibrils (PFFs) were thawed at room temperature immediately before use and diluted to a concentration of 0.1 mg/ml in warm medium and sonicated using a Fisher Scientific Sonicator Dismembrator (Model 100) using a probe tip at 10% power for 30 s (0.5 s on, 0.5 s off). Sonicated fibrils were added to neuronal cultures at 5 DIV at a final concentration of 5 µg/mL for 10–14 days.

Cell death and survival assays

Neuronal apoptosis was measured by visualizing nuclear morphology in Hoechst 33342 stained cells as described previously [31]. Briefly, neurons were fixed using Lana's Fixative (4% paraformaldehyde, 0.2% picric acid) for 30 minutes, washed in PBS and stained with Hoechst 33342 (Invitrogen #H1399) at a concentration of 0.5 µg/mL. The fraction of cells exhibiting an apoptotic nuclear morphology characterized by pyknotic and/or fragmented nuclei containing condensed chromatin was scored by an individual blinded to the treatments and genotypes. Neuronal survival was assessed via Calcein-AM/Ethidium-Homodimer (Live/Dead) staining (Invitrogen #L3224). Calcein-AM (1 µM) and Ethidium Homodimer (3 µM) were diluted in warmed culture media immediately before use and added to neuron cultures for 10 minutes to determine the ratio of live (Calcein-AM positive) to dead (Ethidium Homodimer positive) cells. In both assays, neurons were visualized by fluorescence microscopy (Olympus IX70) and images were captured using a CCD camera (Q-imaging) and Northern Eclipse software (Empix Imaging) by an individual blinded to the sample identity. A minimum of 500 cells from 5 randomly selected fields were analyzed for each treatment condition.

Real-time quantitative RT-PCR

RNA was isolated via Trizol as per the manufacturer's instructions (Invitrogen # 15596018) and 40 ng was used in one-step Sybr green reverse transcription (RT)-PCR protocol (Qiagen #204154). RT-PCR was carried out on a CFX Connect Real Time System (Biorad) and changes in gene expression were determined by the Δ(ΔCt) method using S12 transcript for normalization. Values for qRT-PCR are reported as fold increase in mRNA levels in treated samples relative to paired untreated controls for transcript of interest. To compare transcript levels between wildtype and ATF4−/− neurons at baseline (untreated) we calculated ΔCt relative to corresponding S12 levels. RT-PCR amplifications were carried out as follows: 50 °C for 10 min, 95 °C for 5 min, 95 °C for 10 se, and 60 °C for 30 s. Primer sequences used for amplification are available upon request.

Western blot analysis

To obtain whole-cell lysates, neurons were incubated in RIPA lysis buffer (Millipore Sigma, #R0278) supplemented with phosphatase inhibitor cocktail (Millipore Sigma, #P5726) and protease inhibitor cocktail (Millipore Sigma, #P8340) for 30 min on ice and soluble extract was recovered following centrifugation. Protein concentrations were determined by BCA assay (ThermoScientific, #23225) and 40 µg of protein was separated on 12% SDS-PAGE gels and transferred to PVDF membrane. Membranes were blocked for 1 h at room temperature in 5% skim milk or 5% BSA prepared in TBST (10 mM Tris, 150 mM NaCl, 0.1% Tween 20) and then incubated overnight with primary antibodies against ATF4 (1:5000; Abcam #184909), Cyclophilin B (1:5000; Abcam #178397), Cleaved (active) Caspase3 (1:1000; Cell Signaling Technologies #9661), GFP (1:1000 Invitrogen #A6455), Vinculin (1:1000 Biorad #MCA465GA), Complex I (1:500; Mitosciences #MS604), eIF2a (1:1000; Cell Signaling Technologies #9722) or phospho-eIF2a (1:1000; Cell Signaling Technologies #9721) at 4 °C. Membranes were then washed in TBST and incubated at room temperature with HRP-conjugated goat anti-rabbit or mouse secondary antibodies (1:10,000; BioRad #1706515) for 1 h. Membranes were then washed again and developed via enhanced chemiluminescence (BioRad #1705061). Chemiluminescence signal was detected with a Bio-Rad ChemiDoc MP Imaging System and densitometric measurements were determined using ImageLab software (Bio-Rad). Protein levels were normalized to Cyclophilin B or Vinculin levels from the same samples.

Immunofluorescence

Neurons were washed with ice cold PBS containing Na_3VO_4 (1 mM; Millipore Sigma #S-6508)) and NaF (25 mM; Millipore Sigma # S-6776) and then fixed in Lana's fixative (4% paraformaldehyde, 0.2% picric acid) for 30 min. Neurons were then permeabilized with 0.3% Triton X-100 and blocked in 4% normal goat serum for 1 h and incubated with primary antibodies against MAP2 (1: 500; Abcam #11267), ATF4 (1:100, Cell Signaling Technologies #11815), Tyrosine Hydroxylase (1:500; Millipore Sigma #AB152 or 1:500; Millipore Sigma MAB318), or p-serine 129 α-synuclein (1:500; Abcam #59264) in 2% goat serum/0.3% Triton-X100 in PBS overnight at 4 °C. The next day, cells were washed with PBS and incubated with appropriate Alexa Fluor (Invitrogen) conjugated secondary antibodies in 2% goat serum/0.3% Triton-X100 in PBS for 2 hours at room temperature. Neurons were then washed in PBS and Hoechst stained. Coverslips were mounted onto glass microscope slides (VWR #48311-600) using ProLong Gold mounting medium (Invitrogen #P36930). Images were captured on a Lecia SP8 confocal microscope equipped with LAS X Navigator Software (Leica Microsystems).

ATF4 immunofluorescence quantification

Mesencephalic neurons cultured on coverslips in 4-well dishes were immunostained for ATF4 (CST #11815) and TH (Millipore Sigma MAB318) as described above and

visualized using a Leica SP8 confocal microscope. A minimum of 12 randomly selected TH+ cells per coverslip were identified and marked using LAS X Navigators Software (Leica Microsystems) and then z-stacked images were automatically acquired at ×40 magnification from each dopaminergic neuron using optimized excitation/emission parameters for Hoechst 33342, TH (Alexa-555), ATF4 (Alexa-647). All images were acquired using identical laser settings. ATF4 fluorescence in the nucleus was quantified using the RGB Measure Tool in ImageJ and was recorded as the average pixel intensity per nucleus. A minimum of 12 dopaminergic neurons in each treatment group was analyzed in at least 3 independent experiments (>36 cells per treatment group).

Tyrosine hydroxylase and MAP2 cell counting

Mesencephalic neuron cultures plated on coverslips in 4-well plates were immunostained for tyrosine hydroxylase (Millipore Sigma #AB152) and MAP2 (Abcam #11267) as described above. Neurons were visualized using a Leica SP8 confocal microscope and all TH+ neurons on coverslips were identified using the LAS X Navigator scanning software package (Leica microsystems). The total number of dopaminergic (TH+) cell bodies per coverslip was then scored by an individual blinded to the treatment conditions and survival was determined as the fraction of TH+ cells remaining in treated versus vehicle treated cultures and reported as a percentage. To determine non-DA neuron survival the number of MAP2+/TH− neurons in 5 randomly selected fields per coverslip (minimum of 400 cells per coverslip) was counted by an observer blinded to the sample identity and survival was determined as the fraction of MAP2+/TH− cells remaining in treated versus vehicle treated cultures and reported as a percentage.

Dual TH immunofluorescence and RNAScope fluorescence multiplex in situ hybridization

Mesencephalic neurons cultured on coverslips were fixed for 20 min in Lana's fixative (4% paraformaldehyde, 0.2% picric acid) and dehydrated in ethanol and then coverslips were removed from culture dishes and set face-up on microscope slides (VWR #48311-600) with a surrounding hydrophobic barrier. Cells were then rehydrated and RNAScope multiplex fluorescence (advanced cell diagnostic (ACD) #323136) in situ hybridization was then completed as per manufacturers' instructions. Briefly, slides were incubated in hydrogen peroxide for 10 min then washed with PBS. Cells were then permeabilized with RNAScope Protease III for 10 min at room temperature and washed in PBS. Probe hybridization for CHOP (ACD #317661), Trib3 (ACD #506301), and PUMA (ACD #423721) was carried out for 2 h at 40 °C degrees in a HybEZ II humidity controlled oven (ACD #321720). Probes assigned to individual channels underwent sequential amplification and were then recognized via incubation with HRP and appropriate Opal fluorophores (Akoya Biosciences). Following completion of multiplex in situ hybridization, slides were immunostained for tyrosine hydroxylase as described above and then incubated with DAPI for 30 s and mounted with Prolong Gold mounting medium (Invitrogen #P36930). Cells were visualized using a Leica SP8 confocal microscope and a minimum of 10 randomly selected TH+ cells per coverslip were identified and marked using LAS X Navigator Software and then z-stacked images were automatically acquired from each TH+ neuron at optimized excitation/emission windows for DAPI, TH (Alexa-488), Trib3 (Opal-570), Chop (Opal-620) and Puma (Opal-670). Images for each transcript were individually overlayed on TH/DAPI images and the number of puncta in the soma/nucleus of each TH+ cell was counted manually by an individual blinded to the treatment. A minimum of 10 dopaminergic neurons in each treatment group was scored by an individual blinded to the treatment in at least three independent experiments (>30 cells per treatment group).

Lentivirus Grx1-roGFP2 cloning and production

MitoGrx1-roGFP2 and cytoGrx1-roGFP2 cDNAs were PCR amplified from plasmids pLPCXmitoGrx1-roGFP2 and pLPCX cytoGrx1-roGFP2 using forward primers containing an AgeI restriction site and a reverse primer containing an XbaI restriction site. PCR products were digested and inserted into AgeI/XbaI digested pUltra lentiviral transfer plasmid. The resulting pUltra-mitoGrx1-roGFP2 and pUltra-cytoGrx1-roGFP2 plasmids were transformed and amplified in Stable3 bacterial cells (ThermoFisher #C7373). Lentiviral particles were generated by transfecting HEK293T cells (ATCC CRL-3216) with pUltra-mGrx1-roGFP2 or pUltra-cGrx1-roGFP2 plasmids and the 3rd generation lentiviral packaging plasmids pMDLg/pRRE, pRSV-rev and pMD2.G using Lipofectamine 2000 (ThermoFisher cat #11668027) according to the manufacturers' instructions. Supernatants were collected at 48 h and 72 h post-transfection and cleared by centrifugation and filtration through a 0.45 µm PES syringe filters. Lentiviral particles were concentrated with Lenti-X^{TM} Concentrator (Takara Bio cat #631232) according to the manufacturers' instructions. Lentiviral constructs were then titered in HEK293T cells achieving titers >1 × 10^8 TU/ml. The pLPCXmitoGrx1-roGFP2 (Addgene #64977) and pLPCXcytocGrx1-roGFP2 (Addgene #64975) plasmids were a gift from Dr. Tobias Dick [34]. The pUltra plasmid (Addgene #24129) was a gift from Dr. Malcolm

Moore [35]. The lentiviral packaging plasmids pMDLg/pRRE (Addgene #12251), pRSV-rev (Addgene #12253) and pMD2.G (Addgene #12259) were gifts from Dr. Didier Trono [36]. PCR cloning primer sequences are available upon request.

Ratiometric measurement of glutathione redox in neurons using Grx1-roGFP2 sensors

Neurons were plated at 75,000 cells/well in Nunc 96-well Black-Optical-bottom culture plates (ThermoFisher #165305) and at DIV 3 transduced with lentiviral vectors expressing either mitochondrial targeted mGrx1-roGFP2 or untargeted cGrx1-roGFP2 at 10-MOI. Neurons were then treated 5–7 days post-transduction with vehicle, MPP+ or 6-OHDA. The emission of roGFP2 was measured between 500 and 530 nm after excitation at 405 nm and 488 nm every 30 s in a SpectraMax M5 plate reader (Molecular Devices). The ratio of fluorescence emission at 405/488 nm was then calculated as a function of time using SoftMax Pro Software (Molecular Devices).

Adenovirus expression construct cloning and production

Adenovirus plasmids pShuttle-CBA and pShuttle-CBA-EGFP were generated by PCR amplification of the Chicken β-actin promoter element with or without EGFP cDNA from plasmid pAM/CBA-EGFP using a KpnI linked forward primer and a HindIII linked reverse primer and insertion into KpnI/HindIII digested pShuttle plasmid containing an SV40pA element inserted into the SalI/BglII cloning site. The adenovirus bicistronic shuttle constructs pShuttle-CBA-EGFP-P2A-ATF4 and pShuttle-CBA-EGFP-P2A-ATF4ΔRK were generated by a two-stage cloning process. First, ATF4 or ATF4ΔRK cDNAs were PCR amplified from plasmid pCMV-mATF4 and pCG-ATF4ΔRK, respectively using forward primers containing a BamHI linker and a reverse primer containing an EcoRI linker and inserted into the BamHI/EcoRI digested pUltra vector (Addgene #24129) to generate the bicistronic expression constructs pUltra-EGFP-P2A-ATF4 and pUltra-EGFP-P2A-ATF4ΔRK. In the second stage the EGFP-P2A-ATF4 and EGFP-P2A-ATF4ΔRK cassettes were PCR amplified using forward primer containing a XhoI linker and reverse primers containing HindIII linker and inserted into the XhoI/HindIII site of pShuttle-CBA described above. All constructs were sequenced to confirm sequence accuracy. The pShuttle plasmid (Addgene #16402) was a gift from Dr. Bert Vogelstein, pCMV-ATF4 (Addgene #21845) was a gift from Dr. David Ron, and the pCG-ATF4ΔRK plasmid was a gift from Dr. Kirsty Millar (University of Edinburgh). PCR cloning primer sequences are available upon request.

Generation of adenoviral vectors was performed as described by Luo and colleagues with modifications [37]. Briefly, pShuttle constructs were linearized with PmeI and electroporated into BJ5183-AdEasier-1 cells (Addgene cat #16399) containing the pAdEasy-1 adenovirus backbone. Positive recombinants were identified by PacI digest and recombinant DNA was amplified in Stbl2 bacterial cells (ThermoFisher cat #10268019). Recombinant AdEasy-shuttle plasmids were digested with PacI and transfected into HEK293A cells (ATCC CRL-1573) using Lipofectamine (ThermoFisher cat #11668027) to generate adenovirus particles. After 10–14 days cells were harvested and crude viral lysate was obtained and amplified in successive rounds in HEK293A cells. Amplified viral lysates were then purified by CsCl gradient centrifugation and desalted by dialysis in Slide-A-Lyzer dialysis cassettes with 10,000 MW cutoff (ThermoFisher cat #66380) for at least 24 h and then filtered through 0.22 µm PES syringe filters. Adenovirus preparations were tittered in HEK293 cells using GFP fluorescence to detect transduced cells and titers of ~1×10^{11} pfu/ml were obtained.

Statistical analysis

Data are reported as mean ± standard error of the mean (SEM) from at least three independent experiments. Sample size was estimated using pilot data and power analysis method. Statistical analyses were performed using GraphPad Prism version 8.2 for Mac (GraphPad Software, USA). Statistical significance was determined using two-tailed paired or unpaired Student's *t*-test for individual comparisons, one-way ANOVA followed by Tukey post-hoc test and two-way ANOVA followed by Sidak post-hoc tests for multiple comparisons and differences were considered significant at $P < 0.05$. In Figure Legends, '*n*' value indicates the number of independent experiments and/or the number of mice of each genotype from which cultures were prepared in independent experiments.

Results

PD neurotoxins cause sustained activation of ATF4 and ATF4-dependent induction of pro-death genes Chop, Trib3, and Puma

The neurotoxins 6-hydroxydopamine (6-OHDA) and 1-methyl-4-phenyl-pyridium (MPP+) cause death of dopaminergic (DA) neurons in vitro and in vivo and have been widely used to investigate cellular mechanisms involved in dopaminergic neuron degeneration in PD [38]. These neurotoxins are known to induce mitochondrial dysfunction and to produce ROS that leads to neuronal injury and cell

death [39, 40]. MPP+ and 6-OHDA are actively taken up by the dopamine transporter leading to preferential damage of dopamine neurons [41]. However, it has been reported that these neurotoxins can also be taken up by non-dopaminergic neurons to varying degrees through a number of other transporters, including organic cation transporters, non-specific plasma membrane amine transporters, and potentially other pathways [42–44]. In this study, we used mouse mesencephalic neuron cultures that consist of ~2–5% dopaminergic neurons and ~95% non-dopaminergic neurons, therefore, we conducted a dose-response to determine the relative sensitivity of these neuronal populations to MPP+ and 6-OHDA. Survival of DA and non-DA neurons was assessed by immunostaining for the DA-neuron specific enzyme tyrosine hydroxylase (TH) and the pan-neuronal marker MAP2. As shown in Fig. 1A, DA neurons were significantly more sensitive than non-DA neurons to both neurotoxins. For example, treatment with 25 µM MPP+ induced ~56.5% loss of dopaminergic (TH+) neurons and only a modest 14.3% decrease in MAP2+ non-DA neurons. Similarly, treatment with 5 µM 6-OHDA led to a marked reduction (~55.6%) in TH+ cells but only a modest decrease in MAP2+ non-DA neurons. However, at higher concentrations these toxins also induced significant loss of non-dopaminergic neurons. Consistent with this we and others have reported that at higher concentrations MPP+ and 6-OHDA can induce cell death in primary cortical neuron cultures [45, 46]. Therefore, we incorporated both mesencephalic and cortical neuron cultures at distinct drug concentrations in these studies. To investigate the role of ATF4 in PD, we initially examined whether these PD-mimetics induce ATF4 expression in primary cortical neurons. As shown in Fig. 1B, both MPP+ and 6-OHDA treatments resulted in a robust (>5-fold) increase in ATF4 expression that persisted for at least 16–24 h. Similarly, at concentrations that induce selective loss of DA neurons in mesencephalic cultures MPP+ and 6-OHDA induced a significant increase in ATF4 expression in the nucleus of DA neurons as determined by immunofluorescence (Fig. 1C). ATF4 is a stress responsive transcription factor that during prolonged stress regulates the expression of pro-apoptotic genes [25, 26]. CHOP, Trib3, and PUMA are known to have pro-apoptotic activity and have been previously reported to be induced by PD neurotoxins and to contribute to subsequent neuronal death [47–50]. To determine whether the PD neurotoxin induced expression of these pro-death factors is regulated by ATF4 we treated mesencephalic cultures derived from wildtype and ATF4-deficient littermates with MPP+ or 6-OHDA and then assessed the mRNA levels of Chop, Trib3, and Puma by RNAscope multiplex in situ hybridization combined with TH immunostaining to enable the quantification of these mRNAs specifically in DA neurons. We detected very few of these pro-death transcripts (<1 per cell) in vehicle treated wildtype and ATF4-null neurons (Fig. 1D). However, treatment with MPP+ or 6-OHDA caused a substantial increase in the mRNA levels of Chop, Trib3, and Puma in wildtype DA neurons, but not in ATF4-deficient DA neurons (Fig. 1D). Similarly, we found that MPP+ and 6-OHDA induced the expression of Chop, Trib3, and Puma mRNA in an ATF4-dependent manner in cortical neurons as determined by qRT-PCR (Fig. 1E). Taken together these results indicate that PD neurotoxins induce sustained activation of ATF4 and that this is required for the transcriptional induction of key pro-death target genes in dopaminergic neurons.

ATF4 transcriptional activity is required for PD− neurotoxin induced neuronal apoptosis

It has been reported that ATF4 can regulate the expression of genes involved in redox homeostasis, therefore, we investigated whether there are intrinsic differences in ATF4-deficient neurons that might affect the level of oxidative stress induced by PD neurotoxins. MPP+ and −OHDA have been shown to produce reactive oxygen species (ROS) by interfering with mitochondrial complex-I activity [38]. Therefore, we first sought to determine whether the levels of mitochondrial complex-I differed between wildtype and ATF4-deficient neurons. As shown in Fig. 2A, mitochondrial complex-I levels remain stable following treatment with MPP+ or 6-OHDA over at least an 8 h period. Furthermore, the level of complex-I does not differ between wildtype and ATF4-deficient neurons at baseline or following treatment with PD neurotoxins. Secondly, since ATF4 can regulate the expression of genes involved in glutathione (GSH) metabolism [25], we investigated whether the GSH redox potential differs between wildtype and ATF4-deficient neurons using the ratiometric fluorescence sensor Grx1-roGFP2 that enables dynamic and sensitive determination of glutathione redox potential in live cells [34]. We used both untargeted cGrx1-roGFP2 and mitochondrial targeted mGrx1-roGFP2 to assess mitochondrial specific oxidative processes. Neurons cultured from ATF4+/+ and ATF4−/− littermates were transduced with lentivirus constructs expressing mGrx1-roGFP2 or cGrx1-roGFP2 and the glutathione redox potential was assessed following treatment with PD neurotoxins (Fig. 2C, D). As shown in Fig. 2C, in neurons expressing mGrx1-roGFP2 the addition of MPP+ or 6-OHDA caused a significant increase in oxidized mitochondrial associated roGFP2 indicative of GSH oxidation. However, this response was not significantly different between wildtype and ATF4-deficient neurons indicating that the intrinsic glutathione redox potential is not different in ATF4-deficient neurons. Interestingly, we found a similar response in neurons

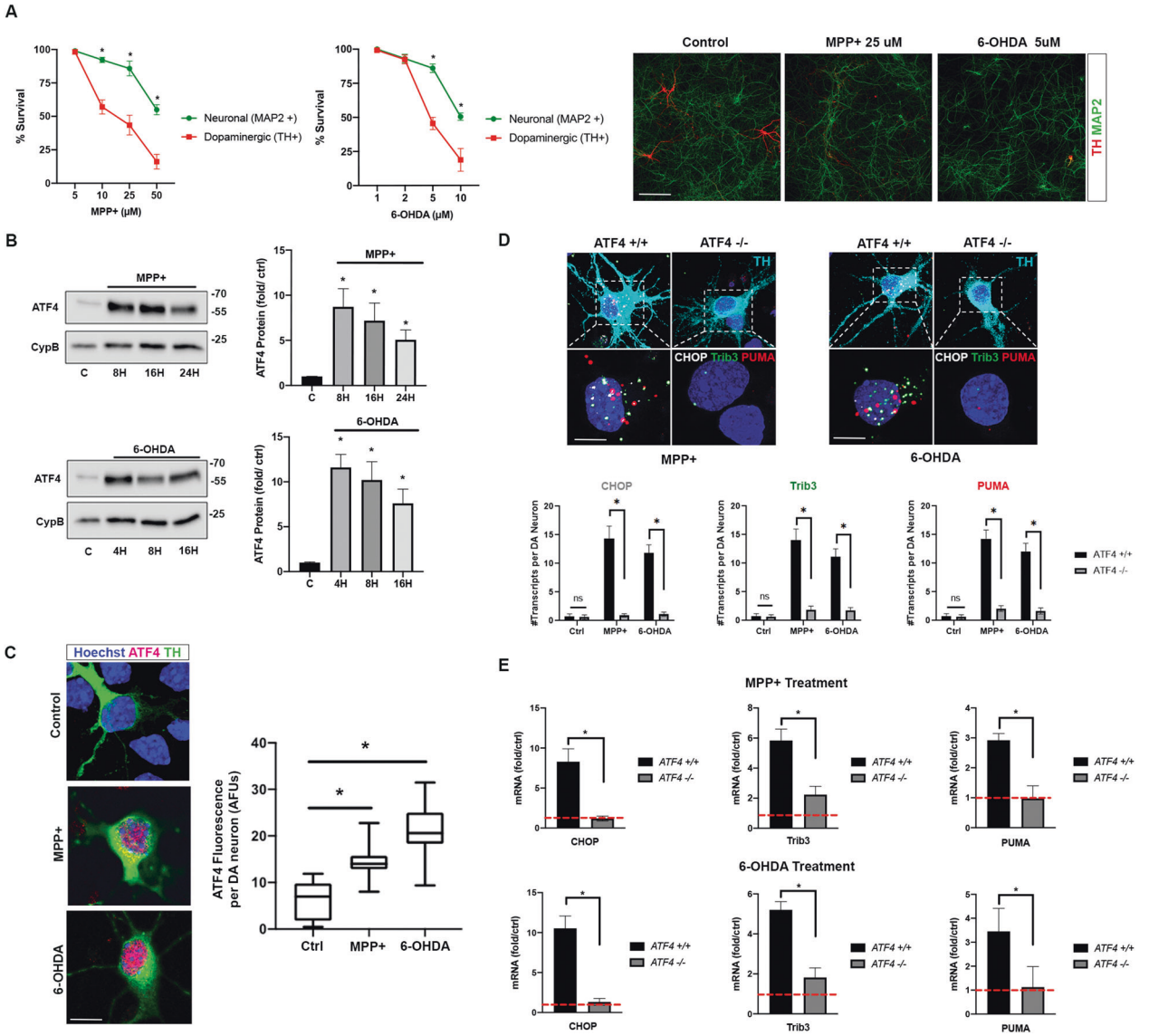

Fig. 1 PD neurotoxins MPP+ and 6-OHDA cause sustained activation of ATF4 and ATF4-dependent induction of pro-death genes Chop. Trib3, and Puma in neurons. A Mesencephalic neuron cultures (7 DIV) were treated with increasing concentrations of MPP+ or 6-OHDA for 48 h and then immunostained for the DA neuron specific marker TH and the pan-neuronal marker MAP2. Representative images of DA neurons (TH, red) and non-DA neurons (MAP2, green) showing preferential loss of DA neurons following treatment with MPP+ and 6-OHDA, scale bar = 100 μm. Survival was determined as the fraction of TH+ (or MAP2+) cells remaining in treated wells as compared with vehicle treated wells and reported as a percentage ($n = 4$; 2-way ANOVA, $^*p < 0.001$). **B** Cortical neurons (7 DIV) were treated with MPP+ (50 μM) or 6-OHDA (10 μM) and at the indicated timepoints ATF4 protein levels were assessed by western blot analysis. Protein levels were quantified by densitometry and ATF4 expression is reported as fold increase over untreated controls following normalization to Cyclophilin B levels ($n = 3$; one-way ANOVA $^*p < 0.05$). **C** Mesencephalic neuron cultures (7 DIV) were treated with MPP+ (25 μM) or 6-OHDA (5 μM) for 12 h and then immunostained for TH and ATF4 and counterstained with Hoechst 33342. Representative images showing induction of ATF4 expression (red) in the nucleus of TH+ dopaminergic neurons (green) following treatment with PD neurotoxins, scale bar = 10 μm. Confocal images were acquired and the fluorescence intensity of ATF4 in the nucleus of TH+ neurons was quantified from a minimum of 36 dopaminergic neurons for each treatment group from three independent experiments (one-way ANOVA, $^*p < 0.01$). **D** Mesencephalic neurons derived from ATF4+/+ and ATF4−/− littermates were treated with vehicle, MPP+ (25 μM) or 6-OHDA (5 μM) for 12 h and then probed for Chop, Trib3, and Puma mRNA levels using RNAscope fluorescence multiplex in situ hybridization and then immunostained for tyrosine hydroxylase. Representative images showing PD neurotoxin induced expression of Chop, Trib3, and Puma mRNA puncta in the soma and nucleus of a wildtype dopaminergic neuron but not in ATF4-null dopaminergic neurons, scale bar = 7.5 μm. The number of transcripts for each target was counted in a minimum of 30 dopaminergic neurons for each treatment group from three independent experiments and data represent the mean ± SEM number of indicated mRNA transcript per DA neuron (ANOVA, $^*p < 0.001$). **E** Cortical neurons derived from ATF4-wildtype and ATF4-null littermates were treated with MPP+ (50 μM) for 16 h or 6-OHDA (10 μM) for 12 h and mRNA levels of indicated transcripts were determine by quantitative RT-PCR. Expression was normalized to S12 mRNA levels and is reported as fold increase over untreated neurons ($n = 4$; unpaired t-test $^*p < 0.01$).

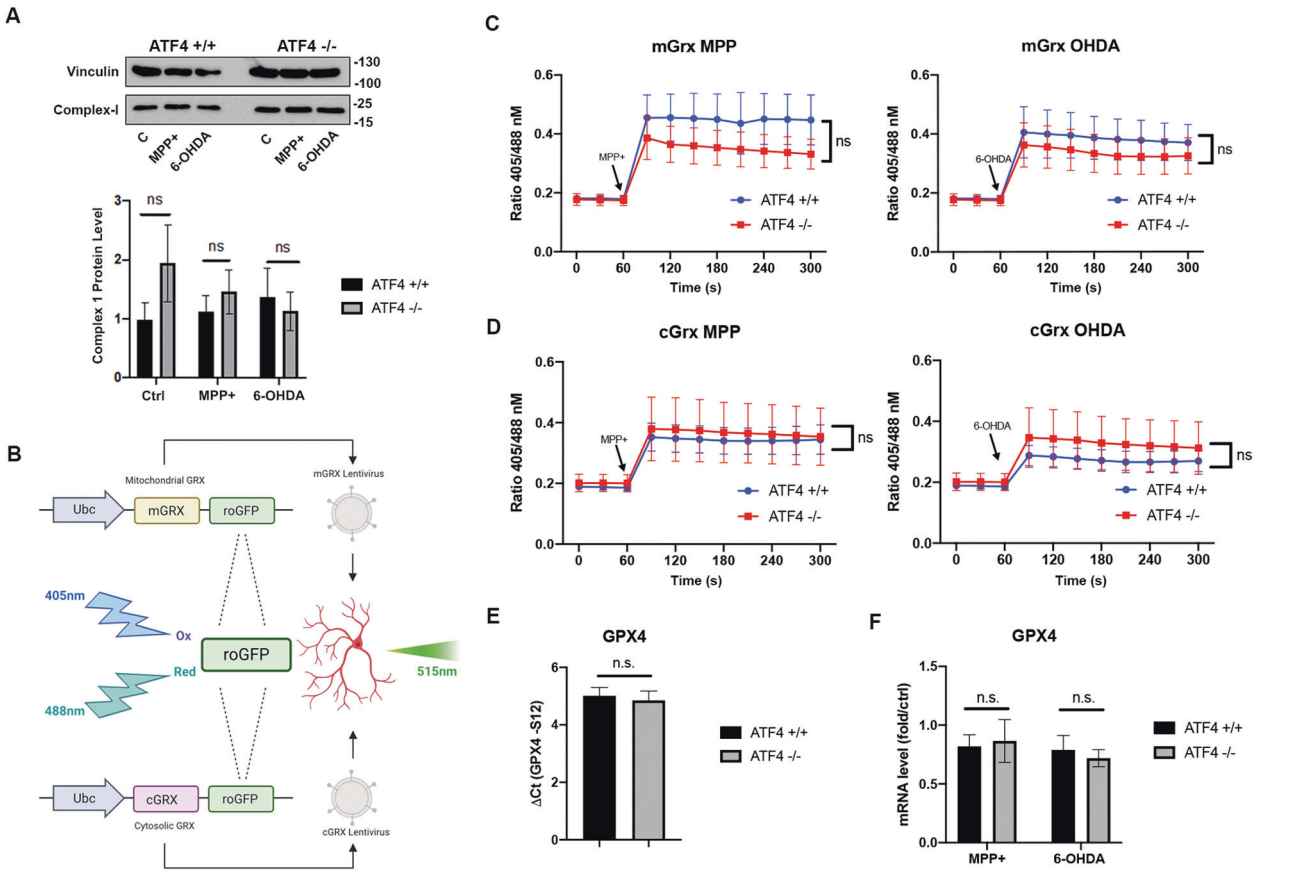

Fig. 2 Effect of ATF4 on PD neurotoxin induced oxidative stress. **A** Cortical neurons derived from ATF4+/+ and ATF4−/− littermates were treated with MPP+ (50 µM) or 6-OHDA (10 µM) for 8 h and mitochondrial Complex-I levels were assessed by western blot analysis. Complex-I levels were quantified by densitometry and normalized to corresponding levels of Vinculin as a loading control ($n = 4$; ANOVA, ns). **B** Schematic of lentivirus Grx1-roGFP2 glutathione redox sensor constructs. **C**, **D** ATF4+/+ and ATF4−/− cortical neurons expressing mGrx1-roGFP2 or cGrx1-roGFP2 were injected with MPP+ (50 µM) or 6-OHDA (10 µM) and the fluorescence emission at 515 nm was measured every 30 s following excitation at 405 nm or 488 nm in a SpectraMax M5 fluorimeter. Data is presented as the ratio of fluorescence emission following excitation at 405 nm/488 nm and represents the mean ± SEM from three independent experiments (two-way ANOVA, ns). **E**, **F** Cortical neurons derived from ATF4 +/+ and ATF4−/− littermates were treated with MPP+ (50 µM) or 6-OHDA (10 µM) for 12 h and mRNA levels of GPX4 was determined by quantitative RT-PCR using S12 mRNA levels for normalization. GPX4 mRNA levels in untreated ATF4+/+ and ATF4−/− neurons was determined by calculating ΔCt (GPX4-S12) ($n = 4$, unpaired t-test, ns) and GPX4 mRNA levels in MPP+ and 6-OHDA treatments was determined by Δ(ΔCt) method and is reported as fold change relative to corresponding untreated neurons ($n = 4$; ANOVA, ns).

expressing non-targeted Grx1-roGFP2 suggesting that PD neurotoxins may also be able to induce oxidative stress in the cytoplasm (Fig. 2D). Although, we cannot rule out the possibility that the ubiquitously expressed cGrx1-roGFP2 can diffuse into the mitochondria and be oxidized by mitochondrial derived ROS. Glutathione Peroxidase-4 (GPX4) catalyzes the reduction of membrane bound phospholipid hydroperoxides and is known to be a key inhibitor of lipid peroxidation induced ferroptosis [51]. PD neurotoxins generate ROS in mitochondria leading to oxidative membrane damage, therefore, we investigated whether ATF4 transcriptionally regulates GPX4 expression in PD toxin paradigms. As shown in Fig. 2E, F, we did not detect a difference in GPX4 mRNA levels between wildtype and ATF4-deficient neurons at baseline or following exposure to MPP+ or 6-OHDA. Furthermore, we did not observe an adaptive increase in GPX4 mRNA expression in these paradigms. This indicates that ATF4 does not regulate the expression level of GPX4 in this context and suggests that any influence ATF4 has on neuronal survival would not be mediated through GPX4 in these PD neurotoxin models.

To determine whether ATF4 expression affects PD neurotoxin induced dopaminergic neuron survival we treated mesencephalic cultures derived from ATF4+/+ and ATF4−/− mice with MPP+ or 6-OHDA and assessed the loss of TH+ cells. As shown, in Fig. 3A, MPP+ treatment resulted in the loss of 63.8% of the DA neurons in ATF4 +/+ cultures as compared to only a 37.1% reduction in ATF4−/− cultures (Fig. 3A). Similarly, 6-OHDA treatment resulted in the loss of 52.4% of the DA neurons in

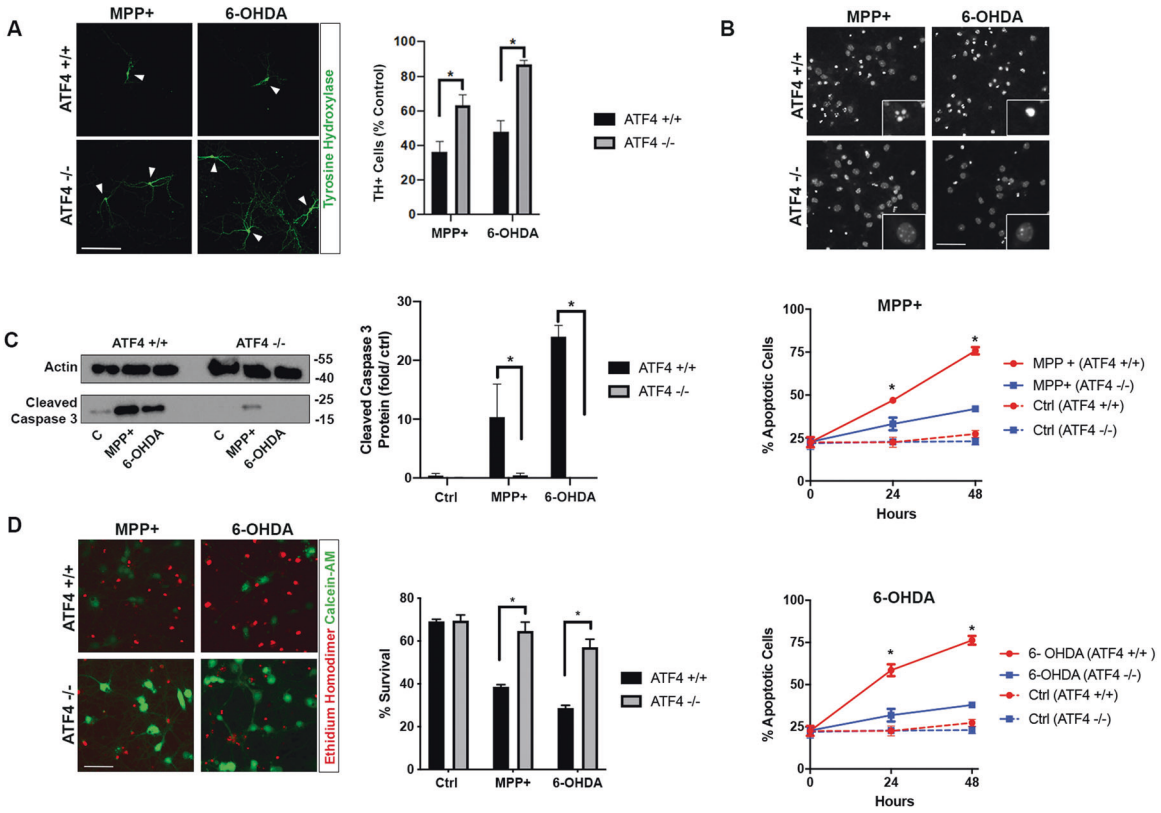

Fig. 3 PD neurotoxin induced ATF4 activation promotes neuronal apoptosis. A Mesencephalic neurons derived from ATF4-wildtype and ATF4-null littermates were treated with MPP+ (25 μM) or 6-OHDA (5 μM) for 48 h and then immunostained for the dopaminergic neuron marker tyrosine hydroxylase. Representative images showing increased numbers of residual dopaminergic neurons (TH+, green) identified by arrows in ATF4−/− mesencephalic cultures as compared to ATF4+/+ cultures following treatment with MPP+ or 6-OHDA. Scale bar = 100 μm. Quantification of the total number of TH+ neurons in ATF4+/+ and ATF4−/− mesencephalic cultures treated with MPP+ (25 μM) or 6-OHDA (5 μM) for 48 h. TH+ cell counts are reported as a percentage of untreated neurons from the same culture. Data represents the mean ± SEM and statistical differences were determined by ANOVA ($n = 4$; $^*p < 0.05$). **B** ATF4+/+ and ATF4−/− cortical neurons were untreated or treated with MPP+ (50 μM) or 6-OHDA (10 μM) and the fraction of apoptotic cells was determined by Hoechst 33342 staining at 0, 24, and 48 h following drug treatment. Data represents the mean ± SEM and statistical differences were determined by two-way ANOVA ($n = 5$; $^*p < 0.01$ between ATF4+/+ and ATF4−/− neurons treated with MPP+ or 6-OHDA). Representative images of Hoechst 33342 stained neurons captured at 48 h following exposure to neurotoxins showing elevated numbers of nuclei exhibiting chromatin condensation and/or nuclear fragmentation in ATF4+/+ cultures as compared to ATF4−/− cultures, scale bar = 50 μm. **C** Cleaved Caspase-3 levels were assessed at 24 h by western blot analysis and quantified by densitometry ($n = 3$; two-way ANOVA $^*p < 0.05$). **D** Neuronal survival was assessed by Calcein-AM/ Ethidium-Homodimer (live/dead) staining at 48 h ($n = 4$; two-way ANOVA $^*p < 0.05$). Representative images of MPP+ and 6-OHDA treated ATF4-wildtype and ATF4-deficient neurons at 48 h using live (green)/dead (red) assay, scale bar = 50 μm.

ATF4+/+ cultures as compared to only a 12.9% reduction in ATF4−/− cultures (Fig. 3A). Dopaminergic neurons make up a small portion of mesencephalic cultures and rapidly lose their TH immunoreactivity as they begin to die making it difficult to assess cell death markers specifically in DA neurons. Therefore, to determine whether PD neurotoxins induce apoptosis and whether this is regulated by ATF4 we treated ATF4+/+ and ATF4−/− cortical neurons with MPP+ or 6-OHDA and then quantified the level of apoptosis as a function of time by assessing nuclear morphology. As depicted in Fig. 3B, treatment of wild-type neurons with MPP+ or 6-OHDA caused a substantial increase in the fraction of cells exhibiting an apoptotic morphology characterized by chromatin condensation and/or nuclear fragmentation. In contrast, in ATF4-deficient neuronal cultures, MPP+ and 6-OHDA treatment resulted in only a modest increase in apoptosis over this same time frame, and the level of apoptosis was found to be significantly lower than in ATF4+/+ neuronal cultures (Fig. 3B). Consistent with the reduction in apoptotic cells we also found that the level of cleaved (active) Caspase-3 induced by MPP+ and 6-OHDA treatments was markedly reduced in ATF4−/− neurons as compared to ATF4+/+ neurons (Fig. 3C). Next to determine whether ATF4-deficient neurons remained viable following treatment with PD− neurotoxins and were not dying by a non-apoptotic mode of cell death we assessed neuronal survival in ATF4+/+ and ATF4−/− neuronal cultures using

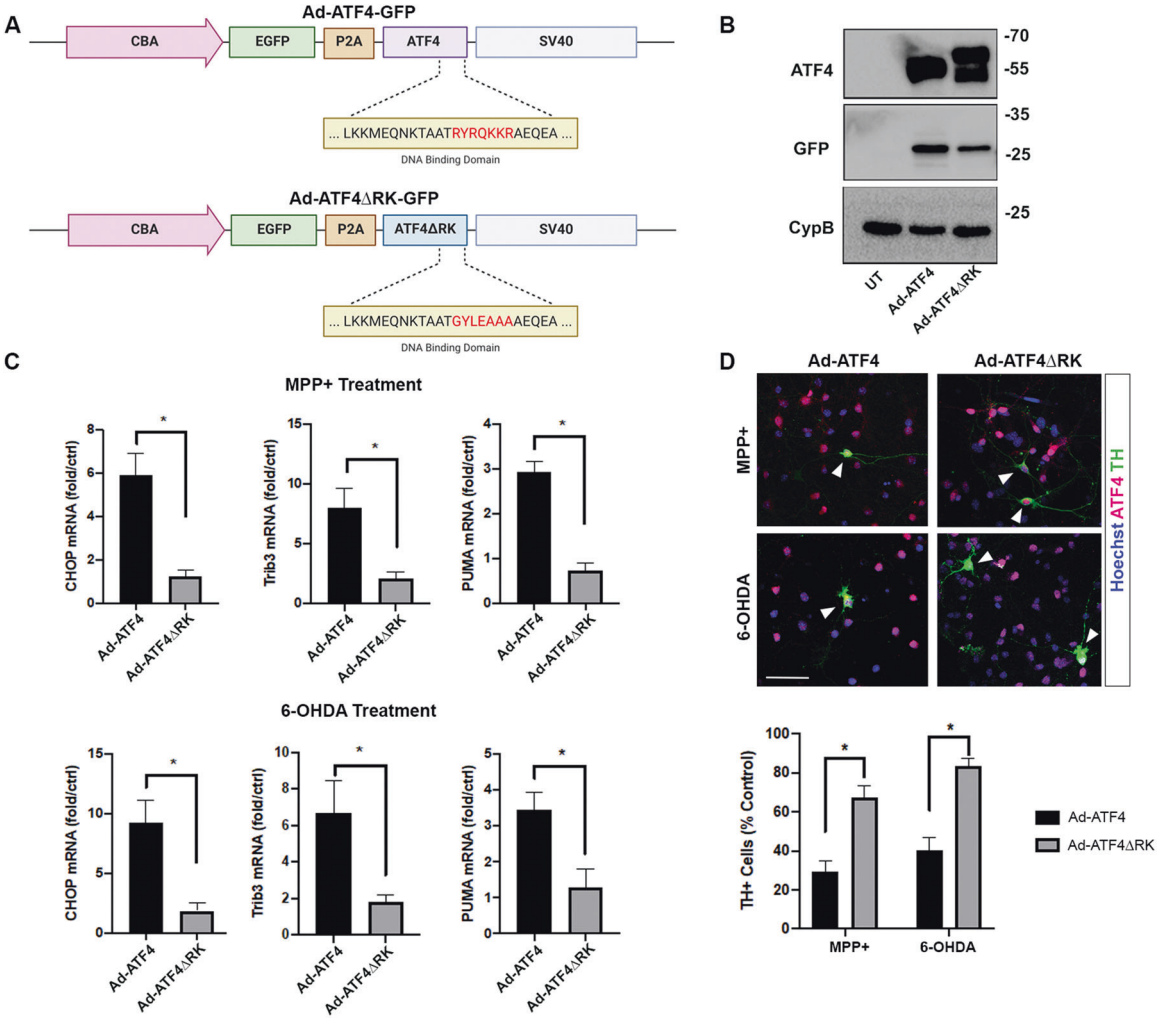

Fig. 4 ATF4 transcriptional activity is required for PD neurotoxin induced dopaminergic neuronal death. A Schematic of adenovirus constructs Ad-GFP-ATF4 and Ad-GFP-ATF4ΔRK that enable bicistronic expression of GFP and either ATF4 or ATF4ΔRK that contains a mutated DNA binding domain rendering it transcriptionally inactive. **B** ATF4-null cortical neurons were transduced at 50-MOI with Ad-GFP-ATF4 or Ad-GFP-ATF4ΔRK for 48 h and the expression of GFP and ATF4 was confirmed by western blot. **C** ATF4−/− cortical neurons were transduced at 50-MOI with Ad-GFP-ATF4 or Ad-GFP-ATF4ΔRK for 36 h. Neurons were then treated with MPP+ (50 μM) or 6-OHDA (10 μM) for 12 h and the mRNA levels of Chop, Trib3 and Puma were determined by qRT-PCR. Expression was normalized to S12 mRNA levels and is reported as fold increase over control ($n = 4$; paired t-test $^*p < 0.05$). **D** Mesencephalic neurons derived from ATF4−/− mice were transduced at 25-MOI with Ad-GFP-ATF4 or Ad-GFP-ATF4ΔRK for 24 h. Neurons were then treated with MPP+ (25 μM) or 6-OHDA (5 μM) and after 48 h neurons were immunostained for ATF4 and the dopaminergic neuron marker tyrosine hydroxylase (TH). Representative images showing Ad-GFP-ATF4 and Ad-GFP-ATF4ΔRK mediated expression of ATF4 (red) in the majority of ATF4-deficient neurons. Images also show decreased numbers of residual dopaminergic neurons (TH+/green) identified by arrows in ATF4−/− mesencephalic cultures transduced with Ad-GFP-ATF4 as compared to Ad-GFP-ATF4ΔRK following treatment with MPP+ or 6-OHDA, scale bar = 50 μm. The number of TH+ neurons was counted for each treatment and is reported as a percentage of the number of TH+ neurons in cultures transduced with Ad-GFP-ATF4 or Ad-GFP-ATF4ΔRK but not treated with PD neurotoxins. Data represent the mean ± SEM and statistical differences were determined by two-way ANOVA ($n = 4$; $^*p < 0.01$).

Calcein-AM/ethidium homodimer staining (Live/Dead assay). As shown in Fig. 3D, MPP+ and 6-OHDA treatments markedly reduced cell viability in ATF4+/+ neurons as compared to ATF4−/− neuronal cultures indicating that ATF4-deficient neurons remain largely viable.

We next wanted to confirm that the transcriptional function of ATF4 is required for promoting PD neurotoxin induced neuronal death. To address this question we transduced ATF4-deficient neurons with recombinant adenoviruses expressing either ATF4 or the transcriptionally inactive DNA binding domain mutant ATF4ΔRK and then treated neurons with MPP+ or 6-OHDA. As shown in Fig. 4C, both MPP+ and 6-OHDA treatments caused a marked increase in Chop, Trib3, and Puma mRNA levels in ATF4-deficient neurons ectopically expressing ATF4, but not ATF4ΔRK. Next, to determine whether ectopic

expression of ATF4 could restore sensitivity of ATF4−/− DA neurons to PD neurotoxins we transduced mesencephalic neuron cultures with Ad-GFP-ATF4 or Ad-GFP-ATF4ΔRK and assessed DA neuron survival. As shown in Fig. 4D, enforced expression of ATF4 but not transcriptionally inactive ATF4ΔRK restored the sensitivity of ATF4-deficient DA neurons to MPP+ and 6-OHDA. The ability of ectopic ATF4 expression but not ATF4ΔRK to restore PD neurotoxin induced death in ATF4-deficient neurons demonstrates that ATF4 transcriptional function is required for its death promoting activity. Furthermore, the ability of enforced ATF4 expression to restore sensitivity rules out the possibility that the observed protection in ATF4-deficient neurons derived from germline knockouts is due to a compensatory effect of ATF4 deletion in these mice.

ATF4 activation by human α-synuclein preformed fibrils promotes neuronal death

We next investigated whether ATF4 regulates neuronal cell death in a cellular model of alpha-synuclein induced pathology. Previous studies have demonstrated that exogenous preformed α-synuclein fibrils (α-Syn PFFs) can be taken up into cultured neurons via endocytosis and induce aggregation of endogenous α-synuclein leading to the formation of intracellular inclusions that in turn, lead to synaptic dysfunction and neuronal death [52]. Synuclein incorporated into pathogenic inclusions is highly phosphorylated at Serine-129 [53]. Therefore, to validate this synucleinopathy paradigm, we treated neurons with α-Syn PFFs for 12 days and confirmed the marked formation of phospho-Ser129-α-synuclein positive inclusions (Fig. 5A). In contrast, neurons treated with vehicle or non-fibrillar α-Synuclein monomers did not exhibit significant levels of phospho-ser129-α-synuclein positive inclusions (Fig. 5A and Supplemental Fig. 1A) consistent with previous reports [52]. As shown in Fig. 5B, α-Syn PFF treated mesencephalic cultures exhibited a significant increase in nuclear ATF4 staining in DA neurons as compared to untreated neurons or cells treated with α-Syn monomers (Fig. 5B and Supplementary Fig. 1B). Next, we treated ATF4+/+ and ATF4−/− mesencephalic cultures with preformed α-synuclein fibrils to examine whether ATF4 induction affects pathogenic α-synuclein induced dopaminergic neuron death. α-Syn PFF induced synucleinopathy resulted in the loss of 81.7% of TH+ dopaminergic neurons in ATF4+/+ cultures, but only a 41.9% reduction in dopaminergic (TH+) neurons in ATF4−/− cultures (Fig. 5C). Consistent with our finding that monomeric (non-fibrillar) α-Syn did not induce phospho-ser129-α-synuclein inclusions, α-Syn monomers had only a modest effect on DA neuron survival (Supplementary Fig. 1C). Previous studies have demonstrated that α-Syn PFFs can also induce toxic aggregates in non-dopaminergic neuronal populations in vitro and in vivo [52, 54, 55]. Consistent with this, we found that α-Syn PFFs also caused a decrease in non-dopaminergic neurons (MAP2+/TH−) in mesencephalic cultures although the extent of this neuronal loss was less than in DA neurons suggesting that DA neurons are more sensitive to α-Syn PFF induced death (Fig. 5C). Similarly, we found that in cortical neuron cultures α-Syn PFFs induced apoptotic cell death to a greater extent in ATF4+/+ than ATF4−/− neurons (Fig. 5D). Having established that α-synuclein PFFs can induce apoptosis and that ATF4 can promote the expression of the pro-apoptotic Bcl-2 family member PUMA we next asked whether PUMA was required for α-syn PFF induced dopaminergic neuronal death. As shown in Fig. 5E, α-syn PFF induced DA neuron loss was markedly reduced in mesencephalic cultures derived from PUMA−/− mice as compared to PUMA+/+ littermates indicating that PUMA is a key effector of α-syn PFF induced DA neuronal death.

The eIF2α kinase inhibitor C16 inhibits ATF4 activation and protects against MPP+ and 6-OHDA induced neuronal death

Given our findings that ATF4 is activated in PD models and promotes neuronal death, we reasoned that pharmacological inhibition of eIF2α kinases that contribute to ATF4 activation in response to oxidative stress and ER stress may be neuroprotective in PD paradigms. In preliminary experiments, we tested inhibitors of different eIF2α kinases and found that the imidazole-oxindole PKR inhibitor commonly known as C16 was able to inhibit ATF4 induction in neurons following treatment with the oxidative stressor sodium arsenite as well as the ER stress inducing agent thapsigargin (Supplementary Fig. 2A). Therefore, we investigated whether C16 could inhibit PD neurotoxin induced ATF4 activation. As shown in Fig. 6A, B, C16 administration significantly reduced the levels of ATF4 induced by MPP+ and 6-OHDA treatments in both cortical neurons and DA neurons in mesencephalic neuronal cultures. Furthermore, we found that the transcriptional induction of Chop, Trb3, and Puma mRNAs induced by MPP + and 6-OHDA was significantly attenuated in the presence of C16 in DA neurons as determined by RNAscope multiplex in situ hybridization (Fig. 6C) and in cortical neurons assessed by quantitative RT-PCR (Supplementary Fig. 2B). Consistent with the ability of C16 to inhibit ATF4 induction and ATF4 transcriptional activity C16 administration markedly reduced the loss of TH+ neurons induced by both MPP+ (61.1 vs 27.6%, $p < 0.05$) and 6-OHDA (43.2 vs 22.9%, $p < 0.05$) (Fig. 6D). Similarly, C16 significantly reduced the level of apoptotic cell death induced by MPP+ and

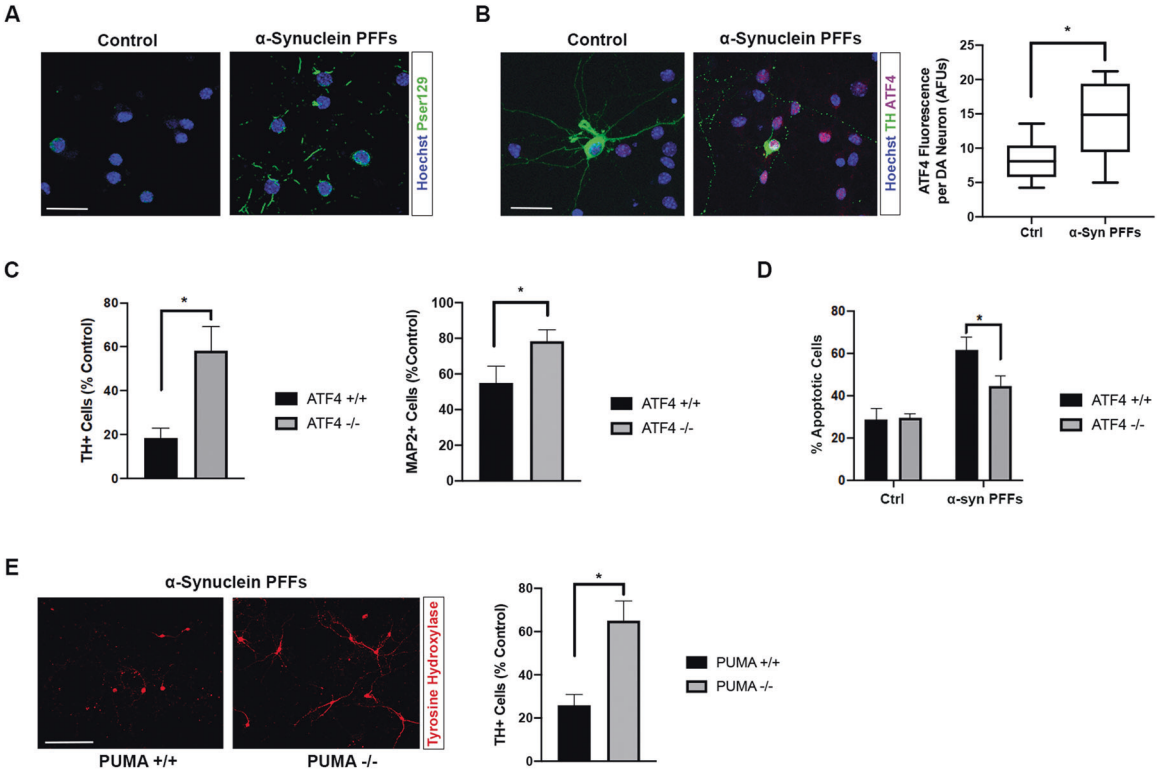

Fig. 5 ATF4 activation by human α-synuclein preformed fibrils promotes neuronal death. A Neurons were treated with α-Syn PFFs (5 µg/ml) or left untreated (control) for 12 days. Representative images showing pathogenic intracellular aggregates of α-Synuclein identified by p-Serine129-α-synuclein immunoreactivity (green), scale bar = 25 µm. **B** Mesencephalic neurons were treated with α-Syn PFFs (5 µg/ml) or left untreated (control) for 12 days and then immunostained for tyrosine hydroxylase (TH) and ATF4. Representative images of ATF4 immunostaining (red) in dopaminergic (TH+) neurons treated with or without α-Syn PFFs, scale bar = 25 µm. Confocal images were acquired and the fluorescence intensity of ATF4 in the nucleus of TH+ neurons was quantified from a minimum of 24 neurons for each group in three independent experiments (paired *t*-test, $*p < 0.01$). **C** Mesencephalic neurons derived from ATF4-wildtype and ATF4-null littermates were treated with or without α-Syn PFFs (5 µg/ml) for 14 days and the number of dopaminergic (TH+) neurons and non-dopaminergic neurons (MAP2+/TH−) was counted and is reported as a percentage of TH+ and MAP2+ cells in untreated controls. Data are shown as mean ± SEM and statistical differences determined by unpaired *t*-test ($n = 3$; $*p < 0.05$). **D** Cortical neurons derived from ATF4-wildtype and ATF4-null littermates were treated with α-Syn PFFs (5 µg/ml) for 14 days and the percentage of apoptotic cells was determined by Hoechst staining. Data are shown as mean ± SEM and statistical differences determined by two-way ANOVA ($n = 4$; $*p < 0.01$). **E** Mesencephalic neuron cultures derived from Puma+/+ and Puma−/− littermates were treated with α-Syn PFFs (5 µg/ml) for 14 days and the number of dopaminergic (TH+) neurons was counted and is reported as a percentage of TH+ cells in untreated Puma+/+ and Puma−/− cultures. Data are shown as mean ± SEM and statistical differences determined unpaired *t*-test ($n = 3$; $*p < 0.05$). Representative images of dopaminergic (TH+) neurons in Puma+/+ and Puma−/− mesencephalic cultures exposed to α-Syn PFFs for 14 days, scale bar = 200 µm.

6-OHDA in cortical neurons (Supplementary Fig. 2C). As shown in Fig. 6E, both MPP+ and 6-OHDA treatments caused a significant increase in the ratio of phosphorylated eIF2α/ total eIF2α. However, C16 did not attenuate PD neurotoxin induced eIF2α phosphorylation suggesting that C16 regulates ATF4 induction independently of PKR or other eIF2α kinases. Therefore, to confirm that the neuroprotective effects of C16 are linked to the attenuation of ATF4 induction, we transduced mesencephalic neurons with Ad-GFP-ATF4 or the control vector Ad-GFP and then treated neurons with MPP+ or 6-OHDA in the presence of C16. As shown in Fig. 6F, ectopic expression of ATF4 reversed the protective effect of C16 on MPP+ and 6-OHDA induced DA neuronal loss indicating that the neuroprotective effect of C16 is indeed mediated by its effects on ATF4 induction.

Discussion

Parkinson's disease is characterized by the loss of dopaminergic neurons, leading to a reduction of dopamine levels, which produce the cardinal motor symptoms of the disease. Unfortunately, the underlying mechanism of neurodegeneration in Parkinson's disease remains poorly understood. In this study, we have demonstrated that ATF4 induction in cellular models of PD promotes neuronal death through transcriptional activation of known pro-death genes

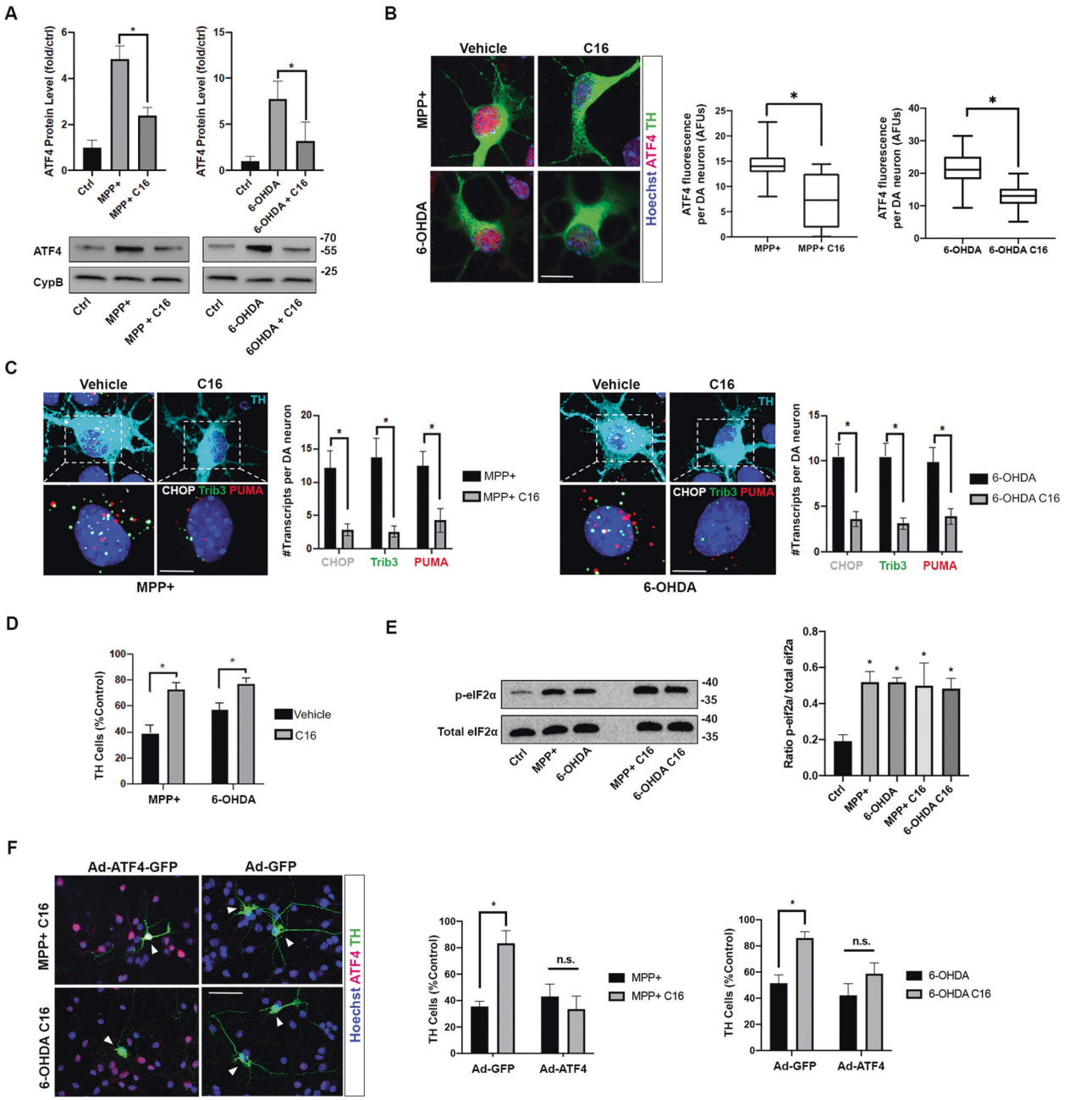

and subsequent apoptotic processes. Specifically, we have determined that (a) ATF4 expression is induced by PD neurotoxins as well as by α-synuclein aggregates produced by preformed α-synuclein fibrils, that (b) ATF4 promotes the expression of the pro-apoptotic target genes Trib3, CHOP, and PUMA, that (c) ATF4-deficient dopaminergic neurons are protected in cellular PD models, that (d) ectopic expression of ATF4 but not transcriptionally defective ATF4ΔRK restores sensitivity of ATF4-deficient neurons to PD neurotoxins and, importantly that (e) pharmacological inhibition of ATF4 attenuates neuronal loss in PD paradigms.

ATF4 is known to induce the expression of genes involved in mitigating cellular stresses but during prolonged activation is also known to induce the expression of pro-apoptotic factors [25, 26]. Consistent with this, ATF4 has been reported to exert both pro-survival and pro-death effects in neurons. Specifically, ATF4 has been reported to promote resistance of HT22 and PC12 cells to glutamate induced oxytosis by inducing the expression of the cystine/glutamate antiporter-xCT [56, 57]. Conversely, in another study it was shown that ATF4-deficient cortical neurons are resistant to cell death induced by hemin or oxidative stress induced by homocysteine mediated glutathione depletion

◀ **Fig. 6 The eIF2α kinase inhibitor C16 inhibits ATF4 activation and protects against MPP+ and 6-OHDA induced neuronal death.** **A** Cortical neurons were treated with MPP+ (50 μM) or 6-OHDA (10 μM) for 8 h in the presence of vehicle or C16 (2 μM) and the level of ATF4 was assessed by western blot analysis and quantified by densitometry. Data represents mean ± SEM and statistical differences determined by one-way ANOVA ($n = 3$; $^*p < 0.05$). **B** Mesencephalic neurons were treated with MPP+ (25 μM) or 6-OHDA (5 μM) in the presence of C16 (2 μM) or vehicle for 12 h and then immunostained for ATF4 and tyrosine hydroxylase. Representative images showing reduced ATF4 (red) expression in the nucleus of dopaminergic (TH+/green) neurons following treatment with PD neurotoxins in the presence of C16, scale bar = 10 μm. Confocal images were acquired and ATF4 fluorescence intensity in the nucleus of TH+ neurons was quantified in a minimum of 30 dopaminergic neurons from three independent experiments (paired *t*-test, $^*p < 0.01$). **C** Mesencephalic neurons were treated with MPP+ (25 μM) or 6-OHDA (5 μM) for 12 h in the presence of C16 (2 μM) or vehicle and then immunostained for TH and probed for Chop, Trib3, and Puma mRNA levels using RNAscope fluorescence multiplex in situ hybridization. Representative images showing that C16 attenuates MPP+ and 6-OHDA induced expression of Chop, Trib3, and Puma mRNA (puncta) in the soma and nucleus of dopaminergic neurons, scale bar = 5 μm. The number of transcripts for each target was counted in a minimum of 30 dopaminergic neurons for each treatment group from three independent experiments and data represents the mean ± SEM number of indicated mRNA transcript per DA neuron (two-way ANOVA, $^*p < 0.05$). **D** Mesencephalic neurons were treated with MPP+ (25 μM) or 6-OHDA (5 μM) for 48 h in the presence of C16 (2 μM) or vehicle and then immunostained for tyrosine hydroxylase (TH). The number of TH+ neurons for each treatment was counted and is reported as the percentage of TH+ cells in corresponding untreated neuronal cultures (two-way ANOVA, $n = 6$; $^*p < 0.05$). **E** Cortical neurons were treated with MPP+ (50 μM) or 6-OHDA (10 μM) in the presence of C16 (2 μM) or vehicle and the levels of p-eIF2α and total eIF2α was assessed at 4 h by western blot. P-eIF2α and total eIF2α levels were quantified by densitometry and data is represented as the ratio of p-eIF2α/ total eIF2α (ANOVA, $n = 4$, $^*p < 0.05$). **F** Mesencephalic neurons were transduced at 25-MOI with Ad-GFP or Ad-GFP-ATF4 for 24 h and then treated with MPP+ (25 μM) or 6-OHDA (5 μM) in the presence of C16 (2 μM) or vehicle for 48 h. Neurons were then immunostained for ATF4 and tyrosine hydroxylase (TH). Representative images showing elevated levels of ATF4 (red) expression in mesencephalic cultures transduced with Ad-ATF4 as compared to Ad-GFP following treatment with PD neurotoxins in the presence of C16, scale bar = 25 μm. Images also show fewer residual TH+ neurons (indicated by arrowheads) in cultures transduced with Ad-ATF4 as compared to Ad-GFP indicating that ectopic expression of ATF4 overrides the neuroprotective effects of C16. The number of TH+ neurons was counted for each treatment and is reported as a percentage of the number of TH+ neurons in cultures transduced with Ad-GFP-ATF4 or Ad-GFP-ATF4ΔRK but not treated with PD neurotoxins (two-way ANOVA, $n = 4$; $^*p < 0.05$).

[58]. Interestingly, this group later characterized hemin and HCA-induced death as ferroptosis suggesting that ATF4 may also play a role in promoting ferroptotic cell death [59]. Furthermore, we have previously demonstrated that ATF4-deficient neurons are resistant to ER stress but not DNA damage induced apoptosis [60]. In the present study, we show that ATF4 functions as a pro-death effector in both neurotoxin and pathological α-synuclein models of PD. Consistent with our findings that ATF4 induction promotes dopaminergic neuronal loss, Gulley and colleagues demonstrated that ectopic expression of ATF4 is sufficient to induce dopaminergic neuron loss in the substantia nigra in vivo [61]. In contrast, it has been reported that in PC12 cells ATF4 expression induces Parkin expression and promotes cell survival in PD toxin paradigms [29]. However, a more recent study by this group demonstrated that Trib3 is induced in cellular models of PD and promotes neuronal death by decreasing Parkin levels in primary neurons [47]. Although our results demonstrate that ATF4 promotes neuronal death in cellular models of PD, future studies will be needed to evaluate the role of ATF4 in in vivo models of PD. However, this will require the generation of brain specific conditional knockout models as adult ATF4 germline knockout mice exhibit peripheral phenotypes including decreased bone mass and microphthalmia and thus are unsuitable for motor or cognitive behavioral testing [30, 62]. Interestingly, ATF4 has been implicated in other neurodegenerative conditions but the mechanisms by which it regulates neuronal loss have yet to be fully understood. Specifically, in Alzheimer's disease, elevated levels of ATF4 has been found in *post-mortem* patient brains, and in mice amyloid-beta causes ATF4 production within axons leading to neurodegeneration [63]. Furthermore, in a mouse model of amyotrophic lateral sclerosis (ALS), ATF4-null transgenic ALS animals exhibited delayed onset of disease and displayed a prolonged lifespan compared ATF4-wild type/ALS animals [64].

In this study, we demonstrated that ATF4 is required for the transcriptional activation of known pro-apoptotic factors CHOP, Trib3, and the Bcl-2 family member PUMA. Interestingly, all three of these factors have previously been reported to contribute to dopaminergic neuronal death in PD neurotoxin models [47–50]. We have determined that PD neurotoxins induce neuronal death, exhibiting characteristics of apoptosis including chromatin condensation and caspase-3 activation and consistent with this the O'Malley lab has reported that dopaminergic neurons derived from Puma-null mice are resistant to MPP+ and 6-OHDA induced death [48, 49]. Interestingly, in the present study, we have found that PUMA is also a key effector of α-Syn PFF induced dopaminergic neuron death. While CHOP and Trib3 have been implicated in neuronal death, the mechanism by which these targets lead to neuronal loss is not completely understood. CHOP and Trib3 have previously been reported to negatively regulate the serine/threonine survival kinase Akt, leading to dephosphorylation and nuclear translocation of different FoxO transcription factors [65–67]. We have previously demonstrated that trophic factor deprivation downregulates Akt and promotes FoxO3a mediated transcriptional activation of PUMA suggesting that these apoptotic factors may be involved in a common apoptotic pathway [68].

The ISR is activated in many neurodegenerative disorders and several studies have investigated the therapeutic potential of targeting eIF2α kinases in mouse models [69, 70]. Related to PD it has recently been reported that PERK signaling is elevated in PD brains and in the SNpc of rodents treated with 6-OHDA [18]. Furthermore, this group demonstrated that administration of the PERK inhibitor GSK2606414 protected nigrostriatal neurons against 6-OHDA induced toxicity and improved motor function. In this study, we found that the PKR inhibitor C16 reduced ATF4 induction and ATF4 mediated transcriptional induction of the pro-apoptotic targets Chop, Trib3, and PUMA. Furthermore, we found that C16 markedly reduced MPP+ and 6-OHDA induced neuronal death and that ectopic expression of ATF4 restored the sensitivity of neurons to PD neurotoxins in the presence of C16, indicating that the protective effects of C16 are mediated by its effect on ATF4 induction. Curiously, while PD neurotoxins induced eIF2α phosphorylation, this was not attenuated by C16, suggesting that C16 regulates ATF4 induction independently of PKR or other eIF2α kinases. Interestingly, it has previously been reported that C16 can exert neuroprotection via PKR-independent mechanisms possibly involving inhibition of CDK5 [71]. Indeed, CDK5 has been implicated in neuronal death in PD models, although whether CDK5 can regulate ATF4 is unknown and will require further investigation [72–74]. Interestingly, the prolyl hydroxylase inhibitor Adaptaquin has been shown to inhibit ATF4 activity through an eIF2α-independent mechanism and very recently Adaptaquin was shown to be protective in cellular models of PD [75, 76].

Acknowledgements This work was supported by grants from the Canadian Institutes of Health Research and the Heart & Stroke Foundation of Canada to SPC and an Ontario Graduate Scholarship to MDD.

Compliance with ethical standards

Conflict of interest The authors declare that they have no conflict of interest.

Publisher's note Springer Nature remains neutral with regard to jurisdictional claims in published maps and institutional affiliations.

References

1. Postuma RB, Berg D, Stern M, Poewe W, Marek K, Litvan I. MDS clinical diagnostic criteria for Parkinson's disease. Mov Disord. 2015;30:1591–9.
2. Damier P, Hirsch EC, Agid Y, Graybiel AM. The substantia nigra of the human brain: II. Patterns of loss of dopamine-containing neurons in Parkinson's disease. Brain . 1999;122:1437–48.
3. Baba M, Nakajo S, Tu PH, Tomita T, Nakaya K, Lee VM, et al. Aggregation of alpha-synuclein in Lewy bodies of sporadic Parkinson's disease and dementia with Lewy bodies. Am J Pathol. 1998;152:879–84.
4. Bosco DA, Fowler DM, Zhang Q, Nieva J, Powers ET, Wentworth P, et al. Elevated levels of oxidized cholesterol metabolites in Lewy body disease brains accelerate a-synuclein fibrilization. Nat Chem Biol. 2006;2:249–53.
5. Bove J, Prou D, Perier C, Przedborski S. Toxin-induced models of Parkinson's disease. J Am Soc Exp Neurother. 2005;2:484–94.
6. Narendra DP, Jin SM, Tanaka A, Suen DF, Gautier CA, Shen J. et al. PINK1 is selectively stabilized on impaired mitochondria to activate Parkin. PLoS Biol. 2010;8:1–21.
7. Clark IE, Dodson MW, Jiang C, Cao JH, Huh JR, Seol JH. et al. Drosophila pink1 is required for mitochondrial function and interacts genetically with parkin. Nature . 2006;441:1162–6.
8. Geisler S, Holmström KM, Treis A, Skujat D, Weber SS, Fiesel FC. et al. The PINK1/Parkin-mediated mitophagy is compromised by PD-associated mutations. Autophagy. 2010;6:871–8.
9. Lee J-Y, Nagano Y, Taylor JP, Lim KL, Yao T-P. Disease-causing mutations in parkin impair mitochondrial ubiquitination, aggregation, and HDAC6-dependent mitophagy. J Cell Biol. 2010;189:671–8.
10. Kaushik S, Cuervo AM. Proteostasis and aging. Nat Med. 2015;21:1406–15.
11. Spillantini GM, Schmidt ML, Lee VM-Y, Trojanowski JQ, Jakes R, Goedert M. a-Synuclein in Lewy bodies. Nature 1997;388:839–40.
12. Michel PP, Hirsch EC, Hunot S. Understanding dopaminergic cell death pathways in Parkinson disease. Neuron. 2016;90:675–91.
13. Mercado G, Castillo V, Soto P, Sidhu A. ER stress and Parkinson's disease: pathological inputs that converge into the secretory pathway. Brain Res. 2016;1648:626–32.
14. Colla E, Coune P, Liu Y, Pletnikova O, Troncoso JC, Iwatsubo T. et al. Endoplasmic reticulum stress is important for the manifestations of α-synucleinopathy in vivo. J Neurosci. 2012;32:3306–20.
15. Heman-Ackah SM, Manzano R, Hoozemans JJM, Scheper W, Flynn R, Haerty W. et al. Alpha-synuclein induces the unfolded protein response in Parkinson's disease SNCA triplication iPSC-derived neurons. Hum Mol Genet. 2017;26:4441–50.
16. Holtz WA, O'Malley KL. Parkinsonian mimetics induce aspects of unfolded protein response in death of dopaminergic neurons. J Biol Chem. 2003;278:19367–77.
17. Hoozemans JJM, van Haastert ES, Eikelenboom P, de Vos RAI, Rozemuller JM, Scheper W. Activation of the unfolded protein response in Parkinson's disease. Biochem Biophys Res Commun. 2007;354:707–11.
18. Mercado G, Castillo V, Soto P, López N, Axten JM, Sardi SP, et al. Targeting PERK signaling with the small molecule GSK2606414 prevents neurodegeneration in a model of Parkinson's disease. Neurobiol Dis. 2018;112:136–48.
19. Ryu EJ, Harding HP, Angelastro JM, Vitolo OV, Ron D, Greene LA. Endoplasmic reticulum stress and the unfolded protein response in cellular models of Parkinson's disease. J Neurosci. 2002;22:10690–8.
20. Slodzinski H, Moran LB, Michael GJ, Wang B, Novoselov S, Cheetham ME. et al. Homocysteine-induced endoplasmic reticulum protein (herp) is up-regulated in parkinsonian substantia nigra and present in the core of Lewy bodies. Clin Neuropathol. 2009;28:333–43.
21. Pakos-Zebrucka K, Koryga I, Mnich K, Ljujic M, Samali A, Gorman AM. The integrated stress response. EMBO Rep. 2016;17:1374–95.
22. Donnelly N, Gorman AM, Gupta S, Samali A. The eIF2α kinases: their structures and functions. Cell Mol Life Sci; 2013;70:3493–511.

23. Lu PD, Jousse C, Marciniak SJ, Zhang Y, Novoa I, Scheuner D, et al. Cytoprotection by pre-emptive conditional phosphorylation of translation initiation factor 2. EMBO J. 2004;23:169–79.
24. Singleton DC, Harris AL. Targeting the ATF4 pathway in cancer therapy. Expert Opin Ther Targets. 2012;16:1189–202.
25. Harding HP, Zhang Y, Zeng H, Novoa I, Lu PD, Calfon M. et al. An integrated stress response regulates amino acid metabolism and resistance to oxidative stress. Mol Cell. 2003;11:619–33.
26. Zinszner H, Kuroda M, Wang XZ, Batchvarova N, Lightfoot RT, Remotti H. et al. CHOP is implicated in programmed cell death in response to impaired function of the endoplasmic reticulum. Genes Dev. 1998;12:982–95.
27. Fawcett TW, Martindale JL, Guyton KZ, Hai T, Holbrook NJ. Complexes containing activating transcription factor (ATF)/cAMP-responsive-element-binding protein (CREB) interact with the CCAAT/enhancer-binding protein (C/EBP)-ATF composite site to regulate Gadd153 expression during the stress response. Biochem J. 1999;339:135–41.
28. Ohoka N, Yoshii S, Hattori T, Onozaki K, Hayashi H. TRB3 a novel ER stress-inducible gene, is induced via ATF4-CHOP pathway and is involved in cell death. EMBO J. 2005;24:1243–55.
29. Sun X, Liu J, Crary JF, Malagelada C, Sulzer D, Greene LA, et al. ATF4 protects against neuronal death in cellular parkinson's disease models by maintaining levels of parkin. J Neurosci. 2013;33:2398–407.
30. Masuoka HC, Townes TM. Targeted disruption of the activating transcription factor 4 gene results in severe fetal anemia in mice. Blood . 2002;99:736–45.
31. Cregan SP, Fortin A, MacLaurin JG, Callaghan SM, Cecconi F, Yu SW. et al. Apoptosis-inducing factor is involved in the regulation of caspase-independent neuronal cell death. J Cell Biol. 2002;158:507–17.
32. Gaven F, Marin P, Claeysen S. Primary culture of mouse dopaminergic neurons. J Vis Exp. 2014;91:e51751.
33. Volpicelli-Daley LA, Luk KC, Lee VMY. Addition of exogenous α-synuclein preformed fibrils to primary neuronal cultures to seed recruitment of endogenous α-synuclein to Lewy body and Lewy neurite-like aggregates. Nat Protoc. 2014;9:2135–46.
34. Gutscher M, Pauleau AL, Marty L, Brach T, Wabnitz GH, Samstag Y. et al. Real-time imaging of the intracellular glutathione redox potential. Nat Methods. 2008;5:553–9.
35. Lou E, Fujisawa S, Morozov A, Barlas A, Romin Y, Dogan Y. et al. Tunneling nanotubes provide a unique conduit for intercellular transfer of cellular contents in human malignant pleural mesothelioma. PLoS ONE. 2012;7:1–11.
36. Dull T, Zufferey R, Kelly M, Mandel RJ, Nguyen M, Trono D. et al. A Third-generation lentivirus vector with a conditional packaging system. J Virol. 1998;72:8463–71.
37. Luo J, Deng ZL, Luo X, Tang N, Song WX, Chen J. et al. A protocol for rapid generation of recombinant adenoviruses using the AdEasy system. Nat Protoc. 2007;2:1236–47.
38. Przedborski S, Ischiropoulos H. Reactive oxygen and nitrogen species: weapons of neuronal destruction in models of Parkinson's disease. Antioxid Redox Signal. 2005;7:685–93.
39. Fallon J, Matthews RT, Hyman BT, Beal MF. MPP+ produces progressive neuronal degeneration which is mediated by oxidative stress. Exp Neurol. 1997;144:193–8.
40. Lotharius J, Dugan LL, O'Malley KL. Distinct mechanisms underlie neurotoxin-mediated cell death in cultured dopaminergic neurons. J Neurosci. 1999;19:1284–93.
41. Wimalasena K. The inherent high vulnerability of dopaminergic neurons toward mitochondrial toxins may contribute to the etiology of Parkinson's disease. Neural Regen Res. 2016;11:246–7.
42. Müller J, Lips KS, Metzner L, Neubert RHH, Koepsell H, Brandsch M. Drug specificity and intestinal membrane localization of human organic cation transporters (OCT). Biochem Pharm. 2005;70:1851–60.
43. Engel K, Wang J. Interaction of organic cations with a newly identified plasma membrane monoamine transporter. Mol Pharm. 2005;68:1397–407.
44. Mapa MST, Le VQ, Wimalasena, K. Characteristics of the mitochondrial and cellular uptake of MPP+, as probed by the fluorescent mimic, 4'I-MPP+. PLoS ONE. 2018;13:e0197946.
45. Steckley D, Karajgikar M, Dale LB, Fuerth B, Swan P, Drummond-Main C. et al. Puma is a dominant regulator of oxidative stress induced bax activation and neuronal apoptosis. J Neurosci. 2007;27:12989–99.
46. Chung Y, Lee J, Jung S, Lee Y, Cho JW, Oh YJ. Dysregulated autophagy contributes to caspase-dependent neuronal apoptosis. Cell Death Dis. 2018;9:1189.
47. Aimé P, Sun X, Zareen N, Rao A, Berman Z, Volpicelli-Daley L, et al. Trib3 Is elevated in Parkinson's disease and mediates death in Parkinson's disease models. J Neurosci. 2015;35:10731–49.
48. Bernstein AI, Garrison SP, Zambetti GP, O'malley KL. 6-OHDA generated ROS induces DNA damage and p53-and PUMA-dependent cell death. Mol Neurodegener. 2011;6:1–13.
49. Bernstein AI, O'Malley KL. MPP+-induces PUMA- and p53-dependent, but ATF3-independent cell death. Toxicol Lett. 2013;219:93–8.
50. Silva RM, Ries V, Oo TF, Yarygina O, Jackson-Lewis V, Ryu EJ. et al. CHOP/GADD153 is a mediator of apoptotic death in substantia nigra dopamine neurons in an in vivo neurotoxin model of parkinsonism. J Neurochem. 2005;95:974–86.
51. Forcina GC, Dixon SJ. GPX4 at the crossroads of lipid homeostasis and ferroptosis. Proteomics . 2019;19:1–11.
52. Volpicelli-Daley LA, Luk KC, Patel TP, Tanik SA, Riddle DM, Stieber A, et al. Exogenous α-synuclein fibrils induce Lewy body pathology leading to synaptic dysfunction and neuron death. Neuron 2011;72:57–71.
53. Fujiwara H, Hasegawa M, Dohmae N, Kawashima A, Masliah E, Goldberg MS, et al. α-Synuclein is phosphorylated in synucleinopathy lesions. Nat Cell Biol. 2002;4:160–4.
54. Wu Q, Takano H, Riddle DM, Trojanowski JQ, Coulter DA, Lee VMY. α-Synuclein (αsyn) preformed fibrils induce endogenous αsyn aggregation, compromise synaptic activity and enhance synapse loss in cultured excitatory hippocampal neurons. J Neurosci. 2019;39:5080–94.
55. Blumenstock S, Rodrigues EF, Peters F, Blazquez-Llorca L, Schmidt F, Giese A, et al. Seeding and transgenic overexpression of alpha-synuclein triggers dendritic spine pathology in the neocortex. EMBO Mol Med. 2017;9:716–31.
56. Lewerenz J, Sato H, Albrecht P, Henke N, Noack R, Methner A, et al. Mutation of ATF4 mediates resistance of neuronal cell lines against oxidative stress by inducing xCT expression. Cell Death Differ. 2011;19:847–58.
57. Lewerenz J, Maher P. Basal levels of eIF2α phosphorylation determine cellular antioxidant status by regulating ATF4 and xCT expression. J Biol Chem. 2009;284:1106–15.
58. Lange P, Chavez J, Pinto J, Coppola G, Sun C, Townes T, et al. ATF4 is an oxidative stress—inducible, prodeath transcription factor in neurons in vitro and in vivo. J Exp Med. 2008;205:1227–42.
59. Zille M, Kumar A, Kundu N, Bourassa MW, Wong VSC, Willis D, et al. Ferroptosis in neurons and cancer cells is similar but differentially regulated by histone deacetylase inhibitors. eNeuro 2019;6:263–81.
60. Galehdar Z, Swan P, Fuerth B, Callaghan SM, Park DS, Cregan SP. Cellular/molecular neuronal apoptosis induced by endoplasmic reticulum stress is regulated by ATF4-CHOP-mediated

induction of the Bcl-2 homology 3-only member PUMA. J Neurosci. 2010;30:16938–48.
61. Gully JC, Sergeyev VG, Bhootada Y, Mendez-Gomez H, Meyers CA, Zolotukhin S, et al. Up-regulation of activating transcription factor 4 induces severe loss of dopamine nigral neurons in a rat model of Parkinson's disease. Neurosci Lett. 2016;627:36–41.
62. Hettmann T, Barton K, Leiden JM. Microphthalmia due to p53-mediated apoptosis of anterior lens epithelial cells in mice lacking the CREB-2 transcription factor. Dev Biol. 2000;222:110–23.
63. Baleriola J, Walker CA, Jean YY, Crary JF, Troy CM, Nagy PL, et al. Axonally synthesized ATF4 transmits a neurodegenerative signal across brain regions. Cell 2014;158:1159–72.
64. Matus S, Lopez E, Valenzuela V, Nassif M, Hetz C. Functional contribution of the transcription factor ATF4 to the pathogenesis of amyotrophic lateral sclerosis. PLoS ONE. 2013;8:1–12.
65. Du K, Herzig S, Kulkarni RN, Montminy M. TRB3: A tribbles homolog that inhibits Akt/PKB activation by insulin in liver. Science. 2003;300:1574–7.
66. Ghosh AP, Klocke BJ, Ballestas ME, Roth KA. CHOP Potentially co-operates with FOXO3a in neuronal cells to regulate PUMA and BIM expression in response to ER stress CHOP potentially co-operates with FOXO3a in neuronal cells to regulate PUMA and BIM expression in response to ER stress. PLoS ONE. 2012;7: e39586
67. Saleem S, Biswas SC. Tribbles pseudokinase 3 induces both apoptosis and autophagy in amyloid-β-induced neuronal death. J Biol Chem. 2017;292:2571–85.
68. Ambacher KK, Pitzul KB, Karajgikar M, Hamilton A, Ferguson SS, Cregan SP. The JNK- and AKT/GSK3β-signaling pathways converge to regulate Puma Induction and neuronal apoptosis induced by trophic factor deprivation. PLoS ONE. 2012;7:1–14.
69. Scheper W, Hoozemans JJM. A new PERKspective on neurodegeneration. Sci Transl Med. 2013;5:1–3.
70. Hugon J, Mouton-Liger F, Dumurgier J, Paquet C. PKR involvement in Alzheimer's disease. Alzheimer's Res Ther. 2017;9:1–10.
71. Chen H-M, Wang L, D'Mello SR. A chemical compound commonly used to inhibit PKR, {8-(imidazol-4-ylmethylene)-6H-azolidino[5,4-g] benzothiazol-7-one}, protects neurons by inhibiting cyclin-dependent kinase. Eur J Neurosci. 2008;28:2003–16.
72. He R, Huang W, Huang Y, Xu M, Song P, Huang Y, et al. Cdk5 inhibitory peptide prevents loss of dopaminergic neurons and alleviates behavioral changes in an MPTP induced Parkinson's disease mouse model. Front Aging Neurosci. 2018;10:162.
73. Qu D, Rashidian J, Mount MP, Aleyasin H, Parsanejad M, Lira A, et al. Role of Cdk5-mediated phosphorylation of Prx2 in MPTP toxicity and Parkinson's disease. Neuron 2007;55:37–52.
74. Wilkaniec A, Czapski GA, Adamczyk A. Cdk5 at crossroads of protein oligomerization in neurodegenerative diseases: facts and hypotheses. J Neurochem. 2016;136:222–33.
75. Karuppagounder SS, Alim I, Khim SJ, Bourassa MW, Sleiman SF, John R, et al. Therapeutic targeting of oxygen-sensing prolyl hydroxylases abrogates ATF4-dependent neuronal death and improves outcomes after brain hemorrhage in several rodent models. Sci Transl Med. 2016;8:328ra29.
76. Aimé P, Karuppagounder SS, Rao A, Chen Y, Burke RE, Ratan RR, et al. The drug adaptaquin blocks ATF4/CHOP-dependent pro-death Trib3 induction and protects in cellular and mouse models of Parkinson's disease. Neurobiol Dis. 2020;136:104725.